Syntaxin 7, syntaxin 8, Vti1 and VAMP7 (vesicle-associated membrane protein 7) form an active SNARE complex for early macropinocytic compartment fusion in *Dictyostelium discoideum*

Aleksandra BOGDANOVIC*, Nelly BENNETT*, Sylvie KIEFFER†, Mathilde LOUWAGIE†, Takahiro MORIO‡, Jérôme GARIN†, Michel SATRE* and Franz BRUCKERT*[1]

*Laboratoire de Biochimie et Biophysique des Systèmes Intégrés, Département de Réponse et Dynamique Cellulaires, CEA-Grenoble, 17 rue des Martyrs, 38054 Grenoble Cedex 9, France, †Laboratoire de Chimie des Protéines, Département de Réponse et Dynamique Cellulaires, CEA-Grenoble, 17 rue des Martyrs, 38054 Grenoble Cedex 9, France, and ‡Institute of Biological Sciences, Gene Experiment Centre, University of Tsukuba, 1-1-1 Ten-nodai, Tsukuba-shi, Ibaraki 305-8572, Japan

The macropinocytic pathway in *Dictyostelium discoideum* is organized linearly. After actin-driven internalization, fluid material passes sequentially from endosomes to lysosomes, where molecules are degraded and absorbed. Residual material is exocytosed via post-lysosomal compartments. Syntaxin 7 is a SNARE (soluble *N*-ethylmaleimide-sensitive fusion protein attachment protein receptor) protein that is present and active in *D. discoideum* endosomes [Bogdanovic, Bruckert, Morio and Satre (2000) J. Biol. Chem. **275**, 36691–36697]. Here we report the identification of its main SNARE partners by co-immunoprecipitation and MS peptide sequencing. The syntaxin 7 complex contains two co-t-SNAREs [Vti1 (Vps10p tail interactor 1) and syntaxin 8] and a v-SNARE [VAMP7 (vesicle-associated membrane protein 7)] (where t-SNAREs are SNAREs of the target compartment and v-SNAREs are SNAREs present in donor vesicles). In endosomes and *in vitro*, syntaxin 7, Vti1 and syntaxin 8 form a complex that is able to bind VAMP7. Antibodies to syntaxin 8 and a soluble recombinant VAMP7 fragment both inhibit *in vitro* reconstituted *D. discoideum* endosome fusion. The lysosomal content of syntaxin 7, Vti1, syntaxin 8 and VAMP7 is low compared with that in endosomes, implying a highly active recycling or retention mechanism. A likely model is that VAMP7 is a v-SNARE present on vesicles carrying lysosomal enzymes, and that the syntaxin 7–Vti1–syntaxin 8 t-SNARE complex is associated with incoming endocytic material.

Key words: endocytosis, macropinocytosis, membrane fusion.

INTRODUCTION

Eukaryotic cells present an amazing variety of endocytic compartments, with intricate membrane traffic pathways linking them together and to the biosynthetic pathway [1]. Lower eukaryotes, such as *Saccharomyces cerevisiae* and *Dictyostelium discoideum*, are therefore favourable model organisms in which to dissect the molecular organization of endocytic traffic because of the reduced number of compartments [2,3]. The macropinocytic pathway of *D. discoideum* appears especially simple, since indigestible fluid-phase markers follow a linear succession of compartments upon internalization. After fluid capture by actin-driven deformation of the plasma membrane [4], the coronin-decorated actin coat disappears rapidly [5], and compartments purified as early as 30 s after internalization already possess endocytic markers, such as the vacuolar ATPase and CP34 cysteine proteinase [6,7]. Plasma membrane recycling occurs within 10 min [8–10]. During this time, endocytosed material is contained in light compartments able to undergo homotypic fusion [11,12], termed endosomes. The density of these compartments increases and a second wave of lysosomal enzyme delivery is discernible [13]. After 15 min, the fluid-phase markers are contained in lysosomes, which are mature, acidic, hydrolytic-enzyme-rich vesicles. Later maturation phases are slower, with macropinocytic compartments acquiring vacuolin B [14,15] and losing lysosomal enzymes [13], while the internal pH concomitantly returns to 6.5. Egestion of undigested material occurs from these post-lysosomal compartments through exocytosis [9,10].

Eukaryotic membrane traffic is regulated by the action of budding and fusion proteins. A precisely timed mechanism of polymerization of coat-forming proteins is controlled by small GTPases of the ADP-ribosylation factor subfamily, and allows selection of cargo and cargo receptors [16]. The fusion mechanism requires the formation of a tight complex between SNAREs {SNAP [soluble NSF (*N*-ethylmaleimide-sensitive fusion protein) attachment protein] receptors}, membrane proteins provided by the fusing compartments [17,18]. The complex consists of a four-helix bundle coiled-coil structure in which three of the helices are provided by two or three t-SNAREs (i.e. SNAREs of the target compartment), and the fourth helix is provided by the v-SNARE (i.e. SNARE present in donor vesicles). The α-helical domains are composed of 57 residues with eight hydrophobic heptad repeats; these are characteristic of SNARE proteins and are known as the t-SNARE motif or the synaptobrevin domain. The activity of SNAREs is tightly regulated, and several priming mechanisms have been proposed, involving small GTPases of the Rab subfamily [19–21]. Additionally, tethering factors define the site of fusion and stabilize the interaction between the SNAREs [19]. Upon fusion, the SNARE complex is dissociated by an active mechanism catalysed by NSF and the SNAPs [22].

Abbreviations used: GST, glutathione S-transferase; GTP[S], guanosine 5′-[γ-thio]triphosphate; HRP, horseradish peroxidase; MALDI–TOF, matrix-assisted laser-desorption ionization–time-of-flight; NSF, *N*-ethylmaleimide-sensitive fusion protein; PNS, post-nuclear supernatant; SNAP, soluble NSF attachment protein; SNAP-25 (-23), synaptosome-associated protein of 25 (23) kDa; SNARE, SNAP receptor; t-SNARE, SNARE of the target compartment; v-SNARE, SNARE present in donor vesicles; Syn7, syntaxin 7; Syn8, syntaxin 8; VAMP, vesicle-associated membrane protein; Vti1, Vps10p tail interactor 1.

[1] To whom correspondence should be addressed (e-mail fbruckert@cea.fr).

The steady-state organization of membrane traffic implies that SNAREs obey special activating and targeting signals [23,24]. For instance, a t-SNARE could reside on a given compartment and possess retention signals, whereas a v-SNARE could shuttle between two compartments and possess alternative targeting signals. Therefore the identification and functional characterization of SNAREs is an essential step in the study of the maturation and vesicular transport mechanisms that shape the endocytic pathway.

In *Dictyostelium*, we have previously identified the general fusion factors NSF, αSNAP and γSNAP [25,26], as well as a syntaxin 7 (Syn7) homologue [27]. Most Syn7 is present in endosomes, where it catalyses their homotypic fusion [27] upon Rab7 activation [11]. In the present work we search for Syn7 SNARE partners.

EXPERIMENTAL

Cell cultures, reagents and general procedures

Dictyostelium discoideum strain Ax-2 was cultivated at 21 °C in shaken suspensions (175 rev./min) in an axenic medium [28]. Exponential-phase growing amoebas (5×10^5 to 1×10^7 cells · ml^{-1}) were harvested by centrifugation (1000 ***g***, 4 min, 4 °C).

Unless specified, biochemical reagents and chemicals were from Sigma or Roche Pharmaceuticals. All DNA constructs were sequenced on both strands. Protein concentration was determined by the BCA assay (Pierce) with BSA as a standard. For Western blot analysis, polypeptides were separated by SDS/PAGE and transferred on to nitrocellulose for immunostaining (Mini Protean II; Bio-Rad). *D. discoideum* Vti1 (Vps10p tail interactor 1), VAMP7 (vesicle-associated membrane protein 7) and syntaxin 8 (Syn8) were detected using rabbit polyclonal antibodies described in the present work (see below). Antibodies to *D. discoideum* Syn7 were described previously [27]. Horseradish peroxidase (HRP)-conjugated secondary antibodies (Bio-Rad) were revealed by enhanced chemiluminescence reagents (ECL®; Amersham Bioscience) and Kodak X-Omat AR film. When needed, the photographic image was digitized using an 8-bit SNAPscan linear densitometer and SNAPWise software. Quantification of proteins of interest was performed with the public domain NIH Image program (developed at the U.S. National Institutes of Health and available on the Internet at http://rsb.info.nih.gov/nih-image/).

The data shown are representative of several independent experiments.

Preparation of soluble His_6–Vti1-(1–193), His_6–VAMP7-(1–190), His_6–Syn8-(1–130) and glutathione transferase (GST)–Syn7-(82–331) recombinant proteins and anti-protein antibodies

Plasmids expressing His_6–Vti1-(1–193), His_6–VAMP7-(1–190) or His_6–Syn8-(1–130) were prepared by inserting a PCR-generated fragment of the SSK661, SSI250 and SSF583 clone respectively into the pQE30 expression vector containing a 5′-polyhistidine coding sequence (Qiagen). Primers were designed to allow in-frame ligation of the PCR product so that the resulting recombinant protein is the portion aa 1–193, aa 1–190 or aa 1–130 of *D. discoideum* Vti1, VAMP7 or Syn8 respectively, fused with an MRGSHHHHHHGS N-terminal extension. GST–Syn7-(82–331) was obtained by excising the *Bam*HI–*Hin*dIII restriction fragment from the His_6–Syn7-(82–331) expression plasmid and inserting it into the pGEX-KG expression vector (Amersham Bioscience).

Escherichia coli M15 (Qiagen) or BL21 (Stratagene) cells were transformed with plasmids expressing His_6–Vti1-(1–193), His_6–VAMP7-(1–190), His_6–Syn8-(1–130) or GST–Syn7-(82–331) and grown in Luria–Bertani medium supplemented with antibiotics according to the manufacturer's recommendations, up to a cell density of $D_{600} = 0.8$. Expression of the recombinant protein was then induced for 2 h at 37 °C with 0.5 mM isopropyl thio-β-D-galactoside (Q-Biogen). Cells were harvested by centrifugation, suspended in lysis buffer (5 mM $MgCl_2$, 50 mM KCl, 2 mM β-mercaptoethanol, 10 μg · ml^{-1} leupeptin, 10 μg · ml^{-1} pepstatin A, 2 μg · ml^{-1} aprotinin, 25 mM Hepes/KOH, pH 7.5) and sonicated. The lysate was then clarified and purified on a 1 ml Ni^{2+}-nitrilotriacetate–agarose column (Qiagen), as described previously for *D. discoideum* His_6–Rab7 [11]. Further purification was performed on a 1 ml DEAE-Sepharose Fast Flow column (Amersham Bioscience) equilibrated in buffer A (25 mM Tris/KOH, pH 8.0, 50 mM NaCl, 1 mM $MgCl_2$, 2 mM β-mercaptoethanol). The proteins of interest eluted in the flowthrough, whereas *E. coli* contaminants were retained. After dialysis against buffer A, the recombinant proteins were concentrated by centrifugation using the Ultrafree system (Millipore) and stored at 4 °C with anti-protease and anti-oxidant reagents (10 μg · ml^{-1} leupeptin, 10 μg · ml^{-1} pepstatin A, 2 μg · ml^{-1} aprotinin, 5 mM β-mercaptoethanol) until use. His_6–VAMP7-(1–190) was quite sensitive to degradation, and was used within 2 weeks.

Portions of 2 mg of purified His_6–Vti1-(1–193), His_6–VAMP7-(1–190) or His_6–Syn8-(1–130) protein were used to raise polyclonal antibodies in rabbits (Elevage scientifique des Dombes, Romans, France). An affinity column was made by coupling 1 mg of the same recombinant protein to glutaraldehyde-activited Affigel-102 resin (Bio-Rad) and used to purify antibodies from rabbit serum as described in [29]. For Western blotting, anti-Vti1 and anti-Syn8 sera were used at a 1:1000 dilution without further purification. The anti-VAMP7 serum, which cross-reacts with His_6–Vti1-(1–193), was passed over a His_6–Vti1-(1–193) affinity column and used at a 1:500 dilution.

In vitro reconstitution of SNARE complexes

GST–Syn7-(82–331) (0.2 or 2 nmol), His_6–Vti1-(1–193), His_6–VAMP7-(1–190) and His_6–Syn8-(1–130) (3 nmol each) were mixed in 115 μl of buffer B (20 mM Tris/HCl, pH 7.5, 50 mM NaCl, 1 mM $MgCl_2$, 7 mM β-mercaptoethanol, 5 μg · ml^{-1} leupeptin, 5 μg · ml^{-1} pepstatin and 2 μg · ml^{-1}aprotinin). After a 72 h incubation at 4 °C, 35 μl of glutathione–Sepharose Fast Flow (Amersham Bioscience) was added and the slurry was further incubated for 1 h at 4 °C. The resin was then washed six times with 1.5 ml of buffer B and recovered by centrifugation (12 min, 20000 ***g***, 4 °C). GST–Syn7-(82–331) and specifically associated polypeptides were eluted in 100 μl of 20 mM glutathione, 100 mM Tris/HCl, pH 8.0, for 30 min at room temperature. Protein material was analysed on an SDS/14 %-PAGE gel. For Western blotting or Coomassie Blue staining, 0.5 or 25 μl of the eluate was loaded respectively.

Preparation of *D. discoideum* post-nuclear supernatant (PNS) and membranes

D. discoideum cells were washed three times in washing buffer (200 mM sucrose, 5 mM glycine/KOH, pH 8.5), suspended at 3×10^8 cells · ml^{-1} in breaking buffer (washing buffer supplemented with 1 mM dithiothreitol, 5 μg · ml^{-1} leupeptin, 5 μg · ml^{-1} pepstatin and 2 μg · ml^{-1} aprotinin) and then broken by six strokes in a ball-bearing cell cracker [30]. A PNS was prepared by centrifugation (1000 ***g***, 5 min, 4 °C). Total cell membranes were obtained by centrifugation of the PNS (100000 ***g***, 30 min, 4 °C; Beckman TL100.3 rotor).

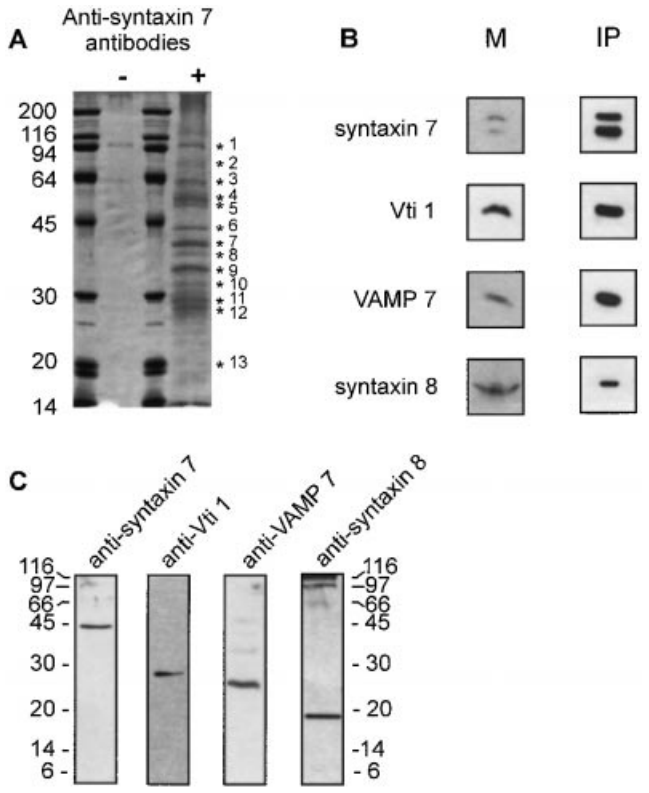

Figure 1 Purification of a set of *D. discoideum* proteins in complex with Syn7

A soluble membrane extract was prepared from 10^9 cells and incubated with anti-Syn7 antibodies coupled to Protein A–agarose (+) or control (−) beads, and specifically associated proteins were revealed as described in the Experimental section. (**A**) Coomassie Blue staining. The purified protein complex corresponds to 5×10^8 cells. Numbers on the right identify polypeptide bands (discussed further in the text). Positions of molecular mass markers (kDa) are indicated on the left. (**B**) Western blot identification of the indicated proteins. Lane M shows the initial membrane extract from 5×10^5 cells, and lane IP shows the immunoprecipitated material from 2×10^7 cells. No polypeptide was detected in the absence of anti-Syn7 antibodies. The relative enrichment of IP compared with M is approx. 20-fold for Syn7 and VAMP7, and 10-fold for Syn8 and Vti1. The lower band for Syn7 corresponds to its degradation product. (**C**) Western blot of total cell extracts with the various antibodies used in this work. A total-cell extract (2×10^5 cells) was separated by an SDS/12%-PAGE gel, transferred on to nitrocellulose and detected by immunostaining with anti-Syn7, anti-Vti1, anti-VAMP7 and anti-Syn8, as described in the Experimental section. Positions of molecular mass markers (kDa) are indicated.

Anti-Syn7 co-immunoprecipitation experiments

Purified polyclonal antibodies (2 mg) raised against His_6–Syn7-(82–331) [26] were coupled to 4 ml of Protein A–agarose beads (Roche) using dimethylsuberimidate [29]. Total *D. discoideum* cell membranes were solubilized in breaking buffer supplemented with 1.6% Triton X-100 and clarified by centrifugation (20000 ***g***, 10 min, 4 °C). A 2 ml aliquot of a soluble membrane extract (corresponding to 5×10^8 cells) was incubated with 150 μl of anti-Syn7-coupled Protein A–agarose beads or Protein A–agarose alone for 2 h at 4 °C. The resins were recovered by centrifugation (10000 ***g***, 10 s, 4 °C). Non-specific binding was removed by a single high-salt wash (200 mM NaCl and 1% Triton X-100 in 1.5 ml of breaking buffer for 15 min). The beads were washed a further three times in 1 ml of breaking buffer supplemented with 1% Triton X-100, resuspended in denaturation buffer and separated by an SDS/PAGE gel for analysis of the protein material.

MS analysis

Electrophoretically resolved protein bands were excised from the gel, washed successively with 25 mM NH_4HCO_3, pH 8.0, and then 50% (v/v) acetonitrile in 25 mM NH_4HCO_3, pH 8.0 (3×15 min). A final wash with pure water was performed before complete dehydration in a vacuum dryer. 'In-gel' tryptic digestion was performed for 4 h at 37 °C in 5–15 μl of 25 mM NH_4HCO_3, pH 8.0, with 0.3–0.5 μg of trypsin per sample, depending on the gel volume and protein amount.

Peptide mass fingerprinting by matrix-assisted laser-desorption ionization–time-of-flight (MALDI–TOF)-MS

Digestion supernatant (0.5 μl) was spotted on to the MALDI sample probe on top of 0.5 μl of a dried mixture made of saturated α-cyano-4-hydroxy-trans-cinnamic acid (Sigma) solubilized in acetone (4 vol.) and nitrocellulose (10 mg/ml), dissolved in 3 vol. of acetone/propan-2-ol (1:1, v/v). Dried samples were rinsed with 5 μl of 0.1% trifluoroacetic acid for 30 s, after which the liquid was blown off by pressurized air. MALDI mass spectra of peptide mixtures were obtained using a Biflex mass spectrometer (Bruker Daltonik). Monoisotopic peptide masses obtained were compared with those calculated for the set of protein sequences deduced from the *Dictyostelium* cDNA database (http://www.csm.biol.tsukuba.ac.jp/cDNA-project.html) using the PeptIdent software (http://au.expasy.org/tools/peptident_dicty.html). When no consistent hit was found, protein identification was achieved by MS/MS analysis.

Peptide sequencing by MS/MS

After in-gel tryptic digestion, gel pieces were extracted first with 5% (v/v) formic acid and then with acetonitrile. The pool of extracts and original digest was dried in a vacuum dryer, redissolved in 10 μl of 10% (v/v) formic acid and desalted using a ZipTip (Millipore). After elution with 5–10 μl of 50% (v/v) acetonitrile/0.1% formic acid, the peptide solution was introduced into a glass capillary (MDS Protana) for nanoelectrospray ionization. Tandem MS experiments were carried out on a Q-TOF hybrid mass spectrometer (Micromass) in order to obtain sequence information. MS/MS sequence information was used for database searching using the programs MS-Pattern (http://prospector.ucsf.edu/) or PeptideSearch located at the EMBL in Heidelberg, Germany.

Sucrose gradient fractionation of *D. discoideum* membranes

To label endosomes, *D. discoideum* cells (10^9 cells per batch) were pulsed for 5 min at 21 °C with 40 μM pyranine in 100 ml of axenic medium. Total cell membranes were prepared, suspended in breaking buffer and layered on to 10 ml linear (25–57%, w/v) sucrose gradients prepared in breaking buffer. After 3 h of centrifugation in a Beckman SW41 rotor at 100000 ***g*** (4 °C), 1 ml fractions were collected from the bottom of the tube. Acid phosphatase and alkaline phosphatase activities were determined using *p*-nitrophenyl phosphate. The pyranine concentration was measured by fluorimetry (450 nm excitation, 510 nm emission), after dilution in 100 mM Tris, pH 10, 0.5% Triton X-100. Proteins of interest were detected and quantified by Western blotting.

Magnetic purification of endocytic compartments

Approx. 10^9 amoebas were incubated for 90 min in 100 ml of axenic medium containing 1.2 mg · ml^{-1} superparamagnetic iron dextran [31] and 40 μM pyranine. A PNS was prepared and

loaded onto a magnetic column [6]. The column was washed in the presence of the magnetic field with 150 ml of breaking buffer, releasing unbound material. The retained material was either batch-eluted in the absence of the magnetic field by gently agitating the iron meshwork in 100 ml of breaking buffer, or fractionated by flowing 100 ml through the column at approx. 1 ml/min. Ten fractions were collected. Half of the retained material was eluted in the fractionation. Membranous and soluble fractions of the retained and non-retained materials were separated by centrifugation. Membranes were then analysed for their iron [32], pyranine and Syn7, Vti1, VAMP7 and Syn8 protein content.

Endosome–endosome fusion assay

Avidin- or biotin–HRP-loaded *D. discoideum* endosomes were prepared and fusion assays were performed as described [11] in the presence of 50 μM guanosine 5′-[γ-thio]triphosphate (GTP[S]), 0.8 mg · ml^{-1} *D. discoideum* cytosol and 10 units · ml^{-1} apyrase as an ATP-depleting system. To test the involvement of Vti1, VAMP7 or Syn8 in endosome fusion, purified antibodies directed against these proteins and/or recombinant His_6-tagged soluble fragments were added to the reaction mixture. As a control, equal volumes of the corresponding buffers were added. Buffers alone were without effect.

RESULTS

Syn7 forms a four-component SNARE complex with Vti1, Syn8 and VAMP7 homologues in *D. discoideum* membranes

In order to identify the Syn7 SNARE partners, purified anti-Syn7 antibodies were coupled with Protein A–agarose beads and incubated with a Triton X-100-solubilized extract of total *D. discoideum* membranes. As a control, Protein A–agarose beads were prepared without anti-Syn7 antibodies. The beads were washed with 0.2 M NaCl to remove most non-specifically adsorbed proteins, and the polypeptides retained on the beads were separated by SDS/PAGE. In the presence of anti-Syn7 antibodies, 13 polypeptides, one of which was a non-specific contaminant, were reproducibly recovered (Figure 1A). As a first approach to identification, all of these protein bands were excised and digested *in situ* with trypsin, and the masses of the trypsin-digested peptides were determined by MALDI–TOF-MS. The peptide mass maps obtained were compared with those calculated for the set of protein sequences from the *Dictyostelium* cDNA database using PeptIdent software. This approach was efficient for nine out of 12 specific polypeptide bands, for which enough peptide masses were generated to permit unambiguous identification (Table 1). This identification was further confirmed either by Western blotting when antibodies were available, or by amino acid sequencing of selected peptides by MS/MS analysis and comparison with the *Dictyostelium* cDNA database (Table 2).

Band 1 was non-specifically associated with the beads, since it was also recovered when anti-Syn7 antibodies were absent. No *Dictyostelium* protein could be assigned to bands 3 and 4. Bands 5 and 10 correspond to two abundant cell proteins, ribosomal α elongation factor and the mitochondrial ADP/ATP translocase respectively. Syn7, the target of the antibodies used, was recovered as a full-length protein (band 6) or a N-terminally shortened fragment (band 7). Three polypeptides represent soluble proteins: NSF (band 2), αSNAP (band 9) and γSNAP (band 8), whose presence is a hallmark of SNARE complexes. The three remaining polypeptides are novel proteins (bands 11, 12 and 13), encoded by the cDNA clones SSK661, SSI250 and SSF583 respectively. FASTA analysis of these polypeptides revealed that they present the characteristic features of the SNARE superfamily: a conserved core domain followed by a single transmembrane helix (Figures 2 and 3A). Like Syn7, the proteins corresponding to the cDNA clones SSK661 and SSF583 contain the 68-residue t-SNARE motif (SMART 00397), while the protein corresponding to clone SSI250 contains the 92-residue synaptobrevin domain (PFAM 00957) (http://www.ncbi.nlm.nih.gov/Structure/cdd/wrpsb.cgi). These three SNAREs are therefore members of the VAMP/synaptobrevin family of v-SNAREs or the Vti/Sec22 family of co-t-SNAREs. Within the 57-residue putative core domains (Figure 3B), the closest mammalian homologues of clones SSK661, SSI250 and SSF583 are human Vti1, VAMP7 and Syn8 respectively (28 %, 38 % and 37 % identity respectively in the core domain). These names will therefore be used hereafter to designate the *D. discoideum* SNAREs. The core domains of Syn7, Syn8, Vti1 and VAMP7 shown in Figure 3(B) were defined from the alignments with their mammalian homologues. The central residue is a Gln (Q) for Syn7, Syn 8 and Vti1 (Q-SNAREs), and an Arg (R) for VAMP7 (R-SNARE) [33].

Table 1 Polypeptide identification by MALDI–TOF-MS in material co-immunoprecipitating with Syn7

Band numbering corresponds to Figure 1(A).

Band no.	Identification
1	Non-specific contaminant
2	NSF
3	Not identified
4	Not identified
5	Elongation factor α
6	Syn7
7	Degraded Syn7
8	γSNAP
9	αSNAP
10	ATP/ADP translocase
11	Vti1
12	VAMP7
13	Syn8

Table 2 Polypeptide identification by MS/MS in material co-immunoprecipitating with Syn7

Band numbering corresponds to Figure 1(A).

Band no.	Identification	No. of peptides identified by MALDI–TOF	Amount of sequence covered (%)	Micro-sequence obtained by MS/MS
11	Vti1	7	30.4	EVENDIDEALK
12	VAMP7	9	39.4	LGVQIPSEFLSDIRIANGNFIDLAR
13	Syn8	2	15.1	ISSTQPYLSDDAR

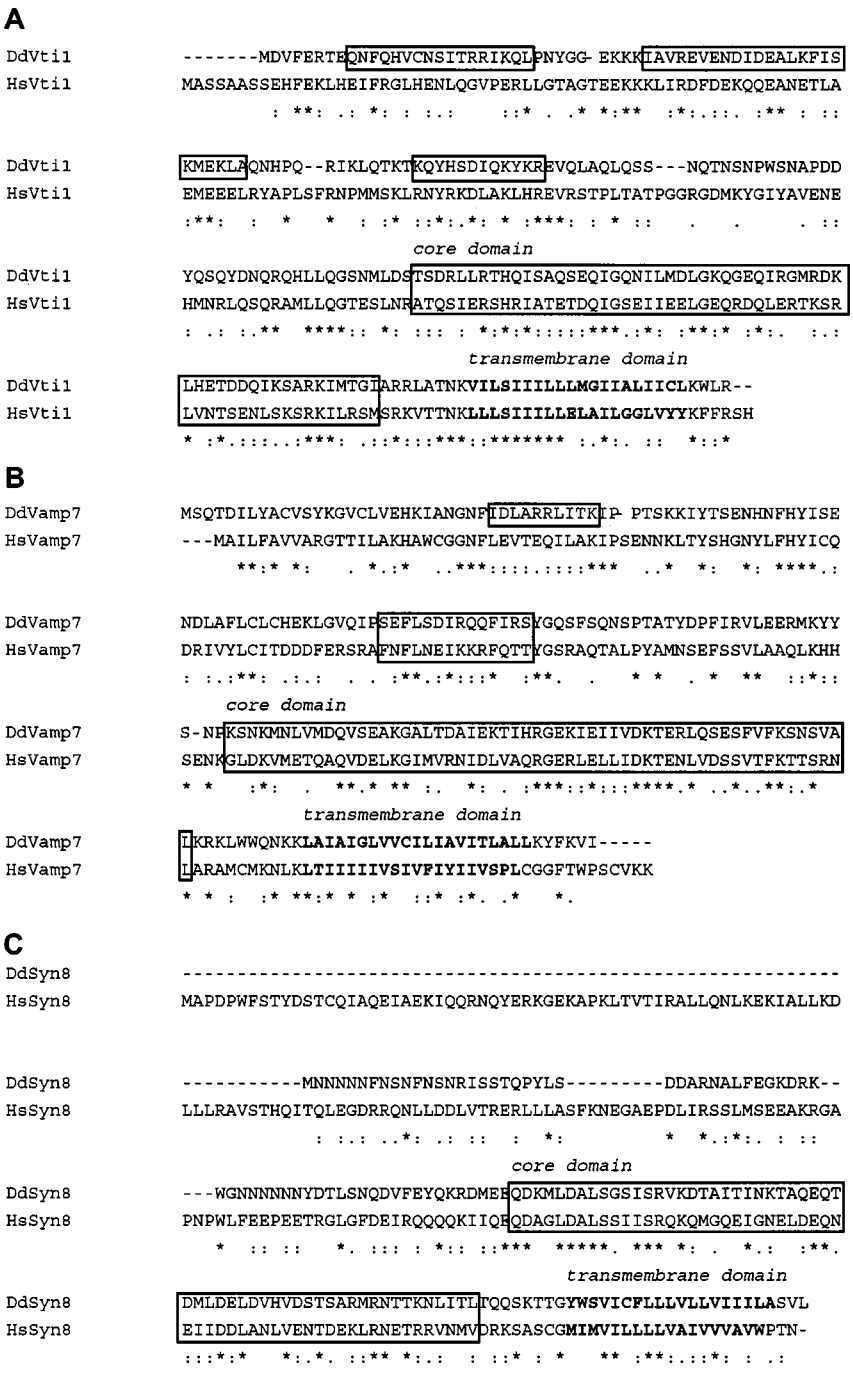

Figure 2 Alignment of *D. discoideum* Vti1, VAMP7 and Syn8 proteins with their human homologues

The *D. discoideum* and human sequences (accession numbers are in given in the legend to Figure 3C) were aligned using the program Clustal W [49]. The transmembrane domains are shown in bold and the core domains are boxed. Other predicted α-helices in *D. discoideum* sequences are also boxed. (**A**) *D. discoideum* (Dd) and *Homo sapiens* (Hs) Vti1; (**B**) *D. discoideum* and *H. sapiens* VAMP7; (**C**) *D. discoideum* and *H. sapiens* syntaxin 8. Asterisks, colons and dots denote identities and strong and weak similarities respectively.

The three SNAREs were expressed as His_6-tagged soluble fragments in *E. coli* and used to raise polyclonal antibodies in rabbits. Each of these antibodies detected one band at the expected molecular size in membrane fractions. They were used to blot 5% of the material recovered with the Protein A–agarose beads in Figure 1(A). The enrichment of Vti1, VAMP7 and Syn8 in the immunoprecipitated fraction compared with the initial material was similar to that of Syn7 (Figure 1B). This confirms that the proteins encoded by clones SSK661, SSI250 and SSF583 co-immunoprecipitate with Syn7, and validates that these antibodies detect Vti1, VAMP7 and Syn8 in membrane extracts. Other SNARE sequences are present in the *Dictyostelium* genomic and cDNA databases which are apparently homologous to Syn7, Vti1, VAMP7 and Syn8. These sequences are designated 'B' isoforms in Figure 3(C) (e.g. DdVamp7B), whereas the sequences forming the immunoprecipitated complex are

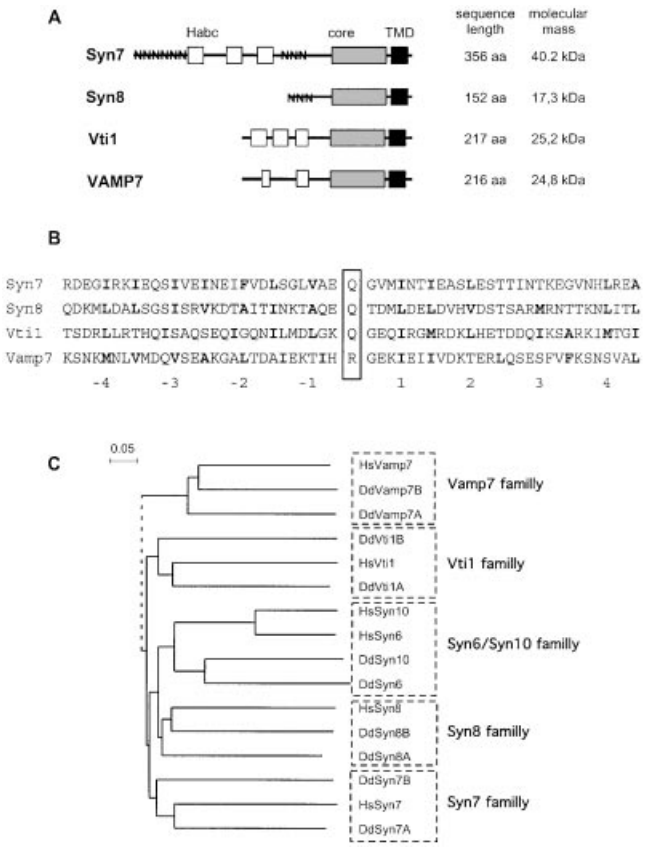

Figure 3 Structure and phylogeny of *D. discoideum* Syn7, Syn8, Vti1 and VAMP7 SNAREs

(**A**) Domain organization of *D. discoideum* Syn7, Syn8, Vti1 and VAMP. The relative sizes of the different parts of the protein are depicted to scale. In white, grey and black are shown the regulatory helices, core domain and transmembrane helices respectively of the four SNAREs. Repetitive regions rich in asparagine are indicated with NNN. (**B**) Alignment of the *D. discoideum* Syn7, Syn8, Vti1 and VAMP7 core domains. The positions of the hydrophobic heptad repeats are shown in bold. The four SNAREs were aligned with their mammalian homologues to delineate the central Q/R position (layer 0), which is boxed [33]. (**C**) Phylogenetic relationship between Syn7, Vti1, Vamp7 and Syn8 homologues in *D. discoideum* and their human counterparts. The protein sequences corresponding to the immunoprecipitated complex were used to scan the human genome. Human homologues of *D. discoideum* Syn7, Vti1, VAMP7 and Syn8 (DdSyn7A, DdVti1A, DdVAMP7A and DdSyn8A respectively) are HsSyn7 (GenBank accession no. AL035306), HsVti1 (AAC52016), HsVAMP7 (AAH20969) and HsSyn8 (AAC95285) respectively. These sequences were used to find similar SNAREs in *Dictyostelium* databases: DdSyn7B (cDNA clone VSJ383; predicted molecular mass 32.8 kDa), DdVti1B (SSM133; 30.5 kDa), DdVAMP7B (SSE713; 29.5 kDa) and DdSyn8B (SSC269; 26.7 kDa). For the sake of completeness, two other DdSyn8A homologues were also found, which are closer to human Syn6 and Syn10: DdSyn6 (U66366), DdSyn10 (SSH272), HsSyn6 (CAA05177) and HsSyn10 (AAC0587). The scale bar indicates the mean number of amino-acid substitutions per sequence position.

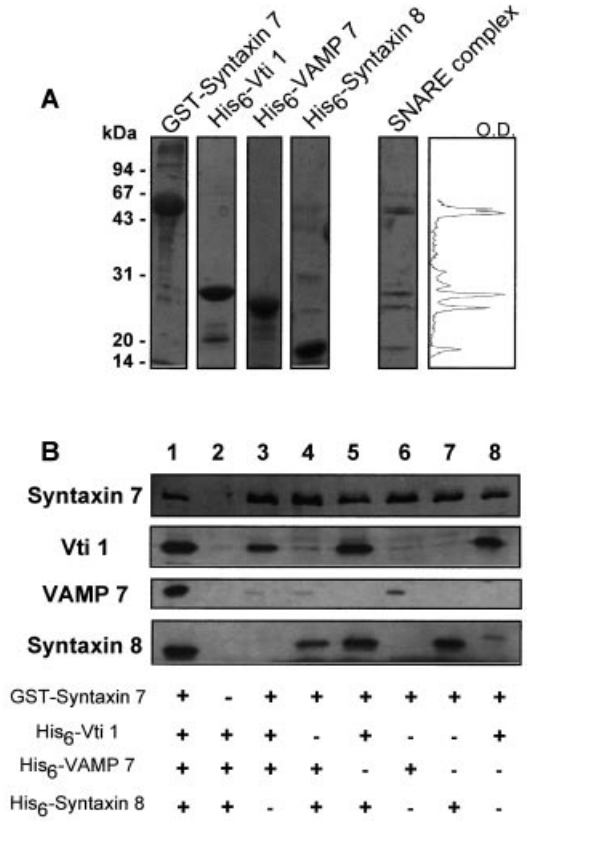

Figure 4 *In vitro* reconstitution of the *D. discoideum* Syn7–Syn8–Vti1–VAMP7 SNARE complex

(**A**) Left: purified GST–Syn7, His_6–Vti1, His_6–VAMP7 and His_6–Syn8. Right: SDS/PAGE analysis of the reconstituted SNARE complex and linear scanning densitometry of the gel (OD, absorbance). The four peaks correspond to GST–Syn7, His_6–Vti1, His_6–VAMP7 and His_6–Syn8, from top to bottom. (**B**) Composition of stable SNARE complexes. Equal amounts of purified GST–Syn7, His_6–Vti1, His_6–VAMP7 and His_6–Syn8 were mixed as indicated, and the SNARE complexes were immobilized and eluted from glutathione–Sepharose as described in the Experimental section. Syn7, Coomassie Blue-stained nitrocellulose; Vti1, VAMP7 and Syn8, Western blot.

designated 'A' isoforms. None of the B isoforms were detected among the proteins co-immunoprecipitated with Syn7. These sequences in fact are not closely related to those of the immunoprecipitated SNARE complex proteins, since the identity between Syn7, Vti1, Vamp7 and Syn8 isoforms is not higher than that between *Dictyostelium* and human sequences ($< 30\,\%$ identity overall). Furthermore, the masses of the polypeptides recognized by the anti-Syn7, anti-Vti1, anti-VAMP7 and anti-Syn8 antibodies correspond to those predicted for clones SSK661, SSI250 and SSF583, and are significantly different from the predicted masses of the B isoforms.

In order to characterize SNARE interactions in the Syn7–Vti1–VAMP7–Syn8 complex, *in vitro* reconstitution experiments were carried out, using the soluble fragments of these proteins (Figure 4). An engineered GST–Syn7 fragment was incubated with equal amounts of the other His_6-tagged SNAREs and the resulting complexes were eluted from glutathione–Sepharose beads (Figure 4A, right). SDS/PAGE analysis revealed the presence of a quasi-equimolar complex between the four SNARE proteins. The modality of its assembly was investigated by testing various SNARE combinations (Figure 4B). In the absence of Syn7, no protein was associated with the resin. Vti1 and Syn8 were able to associate with Syn7 either singly (Figure 4B, lanes 7 and 8) or together (lane 5). In contrast, binding of VAMP7 to Syn7 was greatly enhanced by the simultaneous presence of both Vti1 and Syn8 (compare lanes 3, 4 and 6 with lane 1). These results set VAMP7 apart from Vti1 and Syn8. As expected for co-t-SNAREs, Vti1 and Syn8 associate readily with Syn7, while VAMP7, acting as a v-SNARE, binds only to an already formed three-helix bundle [34,35].

Syn7, Vti1, VAMP7 and Syn8 therefore form a four-component SNARE complex in *D. discoideum* membranes consisting of

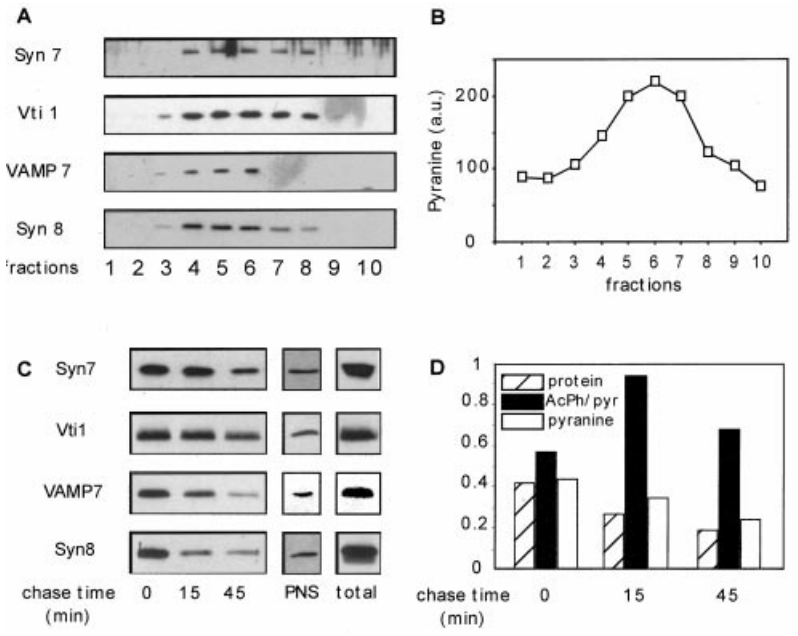

Figure 5 ***D. discoideum*** **Syn7, Vti1, VAMP7 and Syn8 SNAREs co-purify with macropinocytic compartments**

(**A**, **B**) The whole *D. discoideum* macropinocytic pathway was loaded with iron dextran and magnetically purified [6]. Fractions 1–10 correspond to protein material specifically eluting from the magnetic column as the field is removed. (**A**) Western blot of the four SNAREs Syn7, Vti1, VAMP7 and Syn8. (**B**) Elution profile of pyranine, a fluid-phase marker co-internalized with iron dextran. (**C**, **D**) Evolution of the magnetically purified material. Iron dextran and pyranine were internalized for 5 min by *D. discoideum*, then chased for 0, 15 or 45 min or internalized over 1 h ('total'). A PNS was prepared and endocytic compartments were then magnetically purified [6]. (**C**) The presence of the SNAREs was detected by Western blotting. The loaded material corresponds to 3×10^6 cells (0, 15 and 45 min chase time; total) or 2×10^5 cells (PNS). (**D**) Protein concentration (hatched bars), pyranine fluorescence (empty bars) and acid phosphatase activity were determined for the magnetically purified material obtained after a 5 min internalization and a 0, 15 or 45 min chase time (each sample corresponds to an equal number of cells). Solid bars show the ratio of acid phosphatase activity (AcPh) to pyranine concentration (pyr). Units are arbitrary.

one syntaxin (Syn7), two associated t-SNAREs (Vti1, Syn8) and one v-SNARE (VAMP7).

D. discoideum Vti1, VAMP7 and Syn8 homologues are present along with Syn7 in early endocytic compartments

Since the majority of Syn7 is present in *D. discoideum* endosomes [27], we checked for the presence of the other members of the Syn7-containing SNARE complex in the same membranes.

First, we looked for the endocytic localization of these proteins. *D. discoideum* cells were incubated with iron dextran for 1 h to fill up the endocytic compartments, and the endocytic membranes containing iron particles were then purified in a magnetic column. When the magnetic field was removed, specifically retained material was eluted, which was rich in fluid-phase markers and Syn7 [6,27]. Western blotting of the membrane fractions showed that Vti1, VAMP7 and Syn8 co-eluted with Syn7, indicating that the four proteins were present on these membrane compartments (Figure 5A).

A more quantitative estimate of the amounts of these proteins associated with endocytic membranes was obtained by batch elution from the magnetic column (Figure 5C). At least 50%, 49%, 35% and 40% of Syn7, Vti1, VAMP7 and Syn8 respectively was present in the magnetically purified membranes, giving a 5–8-fold relative enrichment (compare 'total' to 'PNS' in Figure 5C). These values compare well with results obtained previously [27]. Furthermore, one should take into account the fact that a substantial fraction of the endocytic compartments is broken during the purification procedure, therefore escaping retention. Approx. 40% of the initially internalized iron dextran is indeed not recovered by sedimentation and flows through the column. Consistent with this interpretation, the Syn7, Vti1, VAMP7 and Syn8 pools not retained on the magnetic column were contained in membranes of low density (results not shown). From these results, we conclude that at least half of the Vti1, VAMP7 and Syn8 in *D. discoideum* is present in or associated with endocytic membranes, as shown for Syn7.

The presence of the four SNARE proteins was checked in endocytic compartments obtained by the magnetic purification technique after pulse–chase internalization of iron dextran (Figure 5C). The amounts of protein and fluid-phase marker recovered decreased slightly with chase time, whereas that of acid phosphatase increased relative to the amount of fluid-phase marker, demonstrating that the nature of the purified compartment is changing towards a more lysosomal character (Figure 5D). Interestingly, SNAREs disappear from the purified compartments with different time courses. Most of the Syn8 and VAMP7 labelling was removed after a 15 min chase, at a time where approx. 40% of Syn7 and Vti1 was still present. After a 45 min chase, only traces of the four SNAREs were recovered in magnetic fluid-containing compartments.

The *D. discoideum* macropinocytic pathway comprises three compartments, i.e. endosomes, lysosomes and post-lysosomes. Most of *Dictyostelium* Syn7 is contained in endosomes [27], which can be separated from other endocytic compartments on sucrose gradients [11,12]. We therefore analysed the distributions of Vti1, VAMP7 and Syn8 on linear 25–57% (w/v) sucrose density gradients (Figure 6). Vti1, VAMP7 and Syn8 exhibited similar fractionation patterns, centred on intermediate-density fractions (fractions 5–8; 30–40% sucrose) containing substantial

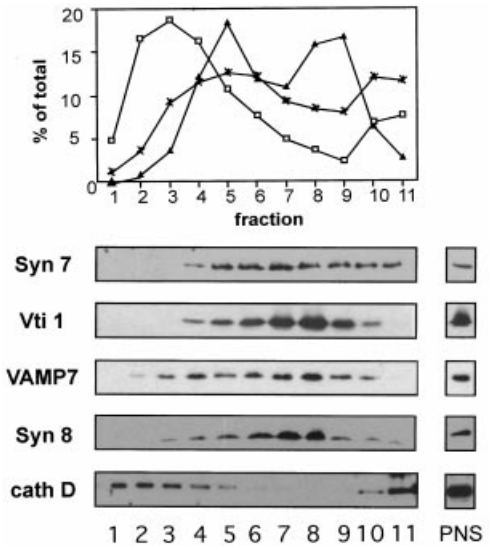

Figure 6 Most of the *D. discoideum* Syn7, Vti1, VAMP7 and Syn8 SNAREs are present in low-density compartments

D. discoideum cells were pulsed for 5 min with pyranine, a fluid-phase marker, to label endosomes. Total *D. discoideum* membranes were prepared and fractionated on a 25–55% (w/v) sucrose gradient as described in the Experimental section. (**A**) Equal volumes of the different fractions were analysed for acid phosphatase (□) or alkaline phosphatase (▲) activity or pyranine content (*), or loaded onto an SDS/12%-PAGE gel. The content of each fraction is normalized to that of the total material. (**B**) Western blot of the indicated proteins along the gradient. The loaded material corresponds to 10^6 cells. PNS indicates the amount of protein contained in 2×10^5 cells. Note that, for cathepsin D (cath D), less protein was recovered on the gradient than expected, in contrast with the SNAREs. This is due to enzyme loss from the compartments broken during the membrane preparation.

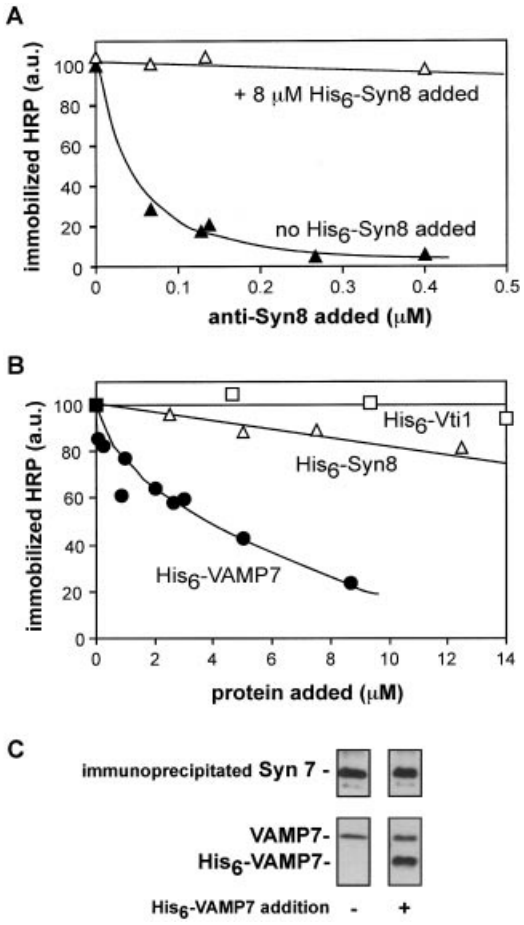

Figure 7 VAMP7 and Syn8 are required for *D. discoideum* endosome–endosome fusion

(**A**, **B**) *In vitro* reconstituted endosome fusion assays carried out in the absence of ATP, as described in [11]. The reactions were preincubated for 15 min on ice before a 45 min incubation at 21 °C. The fusion activity is normalized to that obtained without additions. The solid lines are hand-drawn. (**A**). Anti-Syn8 antibodies inhibit endosome homotypic fusion. The fusion reaction was conducted in the absence (▲) or presence (△) of 8 μM His_6–Syn8 and the indicated amounts of affinity-purified anti-Syn8 antibodies. (**B**) Addition of the soluble His_6–VAMP7 fragment inhibits endosome fusion. The indicated amounts of His_6–VAMP7 (●), His_6–Vti1 (□) or His_6–Syn8 (△) were added to *in vitro* reconstituted endosome fusion assays. (**C**) Binding of His_6–VAMP7 to Syn7 in *D. discoideum* endosomes. Partially purified *D. discoideum* endosomes (2×10^7 cells) were incubated with 5 μM His_6–VAMP7 (+) or control buffer (−) for 1 h at 4 °C in the presence of apyrase (1 unit/ml), cytosol (1 mg/ml), 100 μM GTP[S] and fusion buffer, as in [11]. The membranes were recovered by centrifugation, Syn7 was immunoprecipitated with 10 μl of anti-Syn7 Protein A–agarose beads as described in the Experimental section, and the presence of co-immunoprecipitated VAMP7 was analysed by Western blotting. a.u., arbitrary units.

amounts of Syn7. These fractions are well separated from the lysosomes, which peak at higher densities (fractions 1–4), as indicated by the distribution of cathepsin D and acid phosphatase activity, and from the post-lysosomes, which also sediment at high densities [27]. Therefore the majority of the four SNAREs Syn7, Vti1, VAMP7 and Syn8 is present in membranes of a density similar to that of endosomes. However, it is noteworthy that the distributions of the four SNAREs do not coincide exactly. The Syn7 distribution is centred on fractions 5–7, whereas Syn8 and Vti1 are most abundant in fractions 7–8. The VAMP7 distribution parallels that of Vti1 in fractions 5–10, but extends to compartments of higher densities (fractions 3–4). This is suggestive of the presence of alternative, albeit minor, intracellular localizations for these proteins.

Syn7 co-operates with Vti1, VAMP7 and Syn8 in *D. discoideum* endosome homotypic fusion

The presence of Syn7, Vti1, VAMP7 and Syn8 in similar endocytic membranes suggests that these SNAREs are implicated in a common fusion event involving similar compartments. Using an *in vitro* reconstituted fusion assay, we showed previously that Syn7 mediates endosome–endosome fusion [11]. In this test, avidin- or biotin–HRP-loaded endosomes are mixed in the presence of cytosol and GTP[S] at 21 °C to allow fusion. The resulting avidin–biotin–HRP complexes are immobilized in anti-avidin-coated plates and quantified by HRP enzymic activity.

First, polyclonal antibodies directed against His_6–Vti1 and His_6–Syn8 were affinity purified and added to the endosome fusion assay. Anti-Syn8 antibodies strongly inhibited fusion activity, and this inhibition was reversed by an excess of His_6–Syn8 (Figure 7A). Anti-Vti1 antibodies had no significant effect. Secondly, recombinant soluble fragments of the SNAREs His_6–Vti1, His_6–VAMP7 and His_6–Syn8 were added to the fusion assay in the absence of ATP. His_6–VAMP7 was the most potent, fully inhibiting fusion at micromolar concentrations, Inhibition by His_6–Syn8 was less pronounced, and His_6–Vti1 was without effect (Figure 7B). These data strongly indicate that VAMP7 and Syn8 mediate endosome fusion in *D. discoideum*, along with Syn7. The involvement of Vti1 in the same mechanism is likely, although this was not demonstrated by the reported experiments.

In order to check the specificity of inhibition by the soluble VAMP7 fragment, we probed the functional state of Syn7 on endosomal membranes. The ability of recombinant His_6–VAMP7 to form a complex with Syn7 was tested under conditions allowing its pairing with t-SNAREs and preventing its dissociation (low temperature and absence of ATP). Analysis of the material co-immunoprecipitated with Syn7 revealed the presence of two pools of Syn7 (Figure 7C). A small fraction was associated with endogenous VAMP7, and was therefore insensitive to His_6–VAMP7 addition, while the majority was able to bind an exogenous v-SNARE fragment. The former pool corresponds to previously formed stable *cis*-SNARE complexes, where the v-SNARE is unable to exchange. The latter pool corresponds to free, accessible Syn7, which is able to enter *trans*-SNARE pairing. This is the His_6–VAMP7-sensitive pool. In the absence of His_6–VAMP7, the majority of Syn7 is therefore able to interact with full-length VAMP7 protein, resulting in productive *trans*-SNARE complexes. This pool of Syn7 is likely to be associated with Vti1 and Syn8, which may explain the inability of His_6–Syn8 and His_6–Vti1 to inhibit fusion (Figure 7B).

We therefore conclude that fusion-competent endosome membranes contain unpaired t-SNARE and v-SNARE molecules.

DISCUSSION

Identification of SNARE partners of Syn7 in *D. discoideum*

A four-component SNARE complex was isolated from *D. discoideum* membranes, consisting of a syntaxin and three SNAREs of similar secondary structure. Consistent with the functional nomenclature defined in [34,36], two of these SNAREs (Vti1, Syn8) are co-t-SNAREs that are associated with Syn7 in a t-SNARE complex, whereas the third (VAMP7) is a v-SNARE of the VAMP/synaptobrevin family. The results highlight the remarkable conservation of functional as well as structural differences in co-t-SNAREs and v-SNAREs between *Dictyostelium* and other organisms. First, the three proteins of the t-SNARE complex (Syn7, Vti1 and Syn8) possess a glutamine residue in a medial position of the core complex, whereas VAMP7, the v-SNARE, possesses an arginine. The conservation of *Dictyostelium* VAMP7 and mammalian VAMP8 in the core domain suggests that the structure of the *Dictyostelium* Syn7–Syn8–Vti1–VAMP7 complex is similar to that of the recently published Syn7–Syn8–Vti1–VAMP8 complex [37], in which these four residues are indeed in close contact. Secondly, formation of a t-SNARE complex between Syn7, Syn8 and Vti1 appears to be a prerequisite for the binding of the v-SNARE, and VAMP7 cannot substitute for either Vti1 or Syn8 in this complex (Figure 4).

Vti1, Syn8 and VAMP7 were named by reference to their closest mammalian homologues. Their yeast homologues are respectively Vti1, Vam7 and Nyv1. It should be noted that, despite its name, Syn8 is more closely related to the Vti1/Sec22/Vam7 family than to the syntaxin one. It is also very similar to mammalian syntaxins 6 and 10, and bears 35% identity to human syntaxin 6 in the core domain. Structurally, the absence of a regulatory H_{abc} helical domain (PFAM 00804) clearly distinguishes these proteins from regular syntaxins, such as Syn7. In higher eukaryotes, both VAMP8 and VAMP7 have been shown to interact with Syn7 [38–40]. These v-SNAREs differ in the length of the regulatory domain: VAMP8 is a 'true' synaptobrevin, but VAMP7 is a 'synaptolongin' [41], as is the *Dictyostelium* protein. Interestingly, other putative SNARE protein sequences exist in the *Dictyostelium* genome that are apparently homologous with the immunoprecipitated complex (see the legend of Figure 3C). However, none of the unassigned peptide masses recovered from material co-immunoprecipitated with Syn7 corresponded to these homologues. We therefore conclude that, during vegetative growth, these other SNAREs are not the prominent v- and co-t-SNARE associated with Syn7. Similarly, neither of the two Ykt6 homologues present in the *D. discoideum* EST (expressed sequence tag) database (cDNA clones SSK653 and SSK629) was identified in the Syn7-co-immunoprecipitated complex.

From the co-immunoprecipitation experiment shown in Figure 1(A), roughly equimolar amounts of full-length Syn7, Vti1, VAMP7 and Syn8 were present in the complex. The Syn7 complex was recovered under conditions preventing its dissociation by NSF and SNAP. This complex is likely to correspond to a post-fusion *cis*-SNARE complex that pre-existed before the co-immunoprecipitation procedure. Soluble SNARE fragments are indeed unable to compete with endogenous SNAREs in this complex, although they bind to a sub-pool of Syn7 (Figure 7C). Furthermore, stoichiometric amounts of αSNAP and γSNAP were associated with the complex, while NSF was clearly sub-stoichiometric (compare bands 2, 6, 8 and 9 in Figure 1A). It is quite noteworthy that the 3:1 ratio observed for αSNAP relative to γSNAP in NSF co-immunoprecipitation was also conserved in Syn7 co-immmunoprecipitation, suggesting that γSNAP is a *bona fide* part of the 20 S complex in *D. discoideum* [26].

Membrane traffic of *D. discoideum* Syn7, Vti1, Syn8 and VAMP7

This work provides evidence that these four SNARE partners are present and active in the early part of the *D. discoideum* macropinocytic pathway. The time course of fusion activity closely follows the kinetics of endosome maturation into lysosomes [9,11]. This suggests that the Syn7–Vti1–VAMP7–Syn8 SNARE complex catalyses membrane fusion events allowing the maturation of endosomes into lysosomes. In lysosomes, the route of Syn7, Vti1 and Syn8 separates from that of fluid-phase markers, which proceed to the post-lysosome. Furthermore, Syn7 and Vti1 on the one hand, and Syn8 and VAMP7 on the other, are removed differentially from the lysosomes. This implies the presence of several pathways for the recycling of these molecules.

All of these data are summarized in Figure 8. The t-SNARE complex Syn7–Vti1–Syn8 is present at the plasma membrane and becomes activated upon incorporation into newly formed endosomes. VAMP7 carries the first wave of enzymes (possibly vacuolar ATPase, CP34) either newly synthesized or coming from a recycling compartment. Rab7 activation triggers fusion activity on both compartments, resulting in heterotypic and homotypic fusions [11], providing newly formed endocytic compartments with the hydrolytic content required to digest the internalized material [13]. Then NSF, αSNAP and γSNAP dissociate this complex. The v-SNARE VAMP7 rapidly shuttles back to a reservoir, while the t-SNARE partners return to the plasma membrane. Thus endocytic SNARE recycling occurs in several waves.

The general significance of Syn7, Syn8 and Vti1 as t-SNARE markers for content degradation and VAMP7 as a v-SNARE carrier of lysosomal enzymes is consistent with data obtained in mammalian cells. First, the existence of a physiological complex formed by the same t-SNAREs and VAMP7 [38,39] or VAMP8 [38,42] has been reported in various mammalian cells. Secondly, Syn7, Syn6 (closely related to Syn8) VAMP7, VAMP8 and Vti1 are found on late endosomes and lysosomes [38,39] and partially co-localize [39,43,44]. Thirdly, these SNAREs are involved in late-endosome or lysosome homotypic fusion, as well as late-

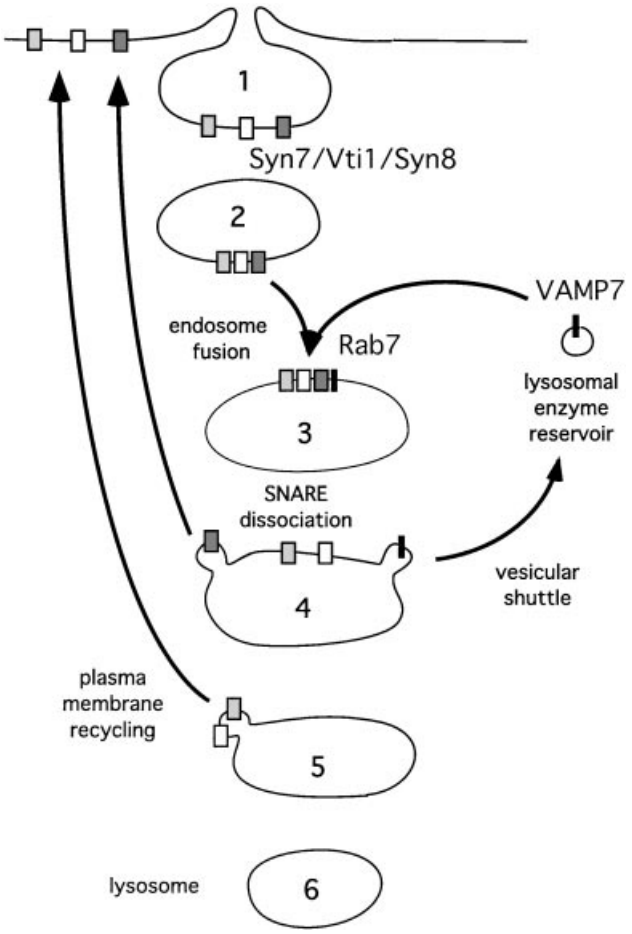

Figure 8 Proposed organization of Syn7, Syn8, Vti1 and VAMP7 traffic in *D. discoideum* phagocytic or macropinocytic pathways

This Figure depicts the proposed roles for the t-SNARE complex (Syn7, Vti1, Syn8) and the v-SNARE VAMP7 in the organization of the *D. discoideum* phagocytic or macropinocytic pathways of eukaryotic cells, on the basis of the current view of endocytic pathway machinery [1]. Step 1, the inactive t-SNARE complex is internalized at the plasma membrane; step 2, priming of the t-SNARE complex in endosomes; step 3, several rounds of membrane fusion, allow mixing of endosome contents together and with lysosomal enzyme-containing vesicles bearing primed VAMP7; step 4, VAMP7 is recycled rapidly back to the lysosomal enzyme reservoir; step 5, the t-SNARE complex is recycled to the plasma membrane; step 6, the internalized material is digested.

endosome–lysosome heterotypic fusion [39,40,42]. In addition, it is worth mentioning that, in neuronal or PC12 cells, VAMP7 (TI-VAMP) localizes to a specialized tubulo-vesicular membrane compartment involved in neurite outgrowth [45]. This cell-specific VAMP7 activity corresponds to the formation of another SNARE complex involving SNAP-25 (synaptosome-associated protein of 25 kDa) [46]. Similarly, VAMP7 is involved in different vesicular transport processes, such as degranulation and apical delivery, possibly in a complex with SNAP-23 and syntaxin 3 [47,48]. In *D. discoideum*, this role for a VAMP7 protein in the exocytic pathway may be fulfilled by the second VAMP7 homologue expressed.

We thank Dr Thierry Soldati for helpful discussions. This work was supported by the Commissariat à l'Energie Atomique, the Centre National de la Recherche Scientifique and the Joseph Fourier University (Grenoble, France).

REFERENCES

1 Gu, F. and Gruenberg, J. (1999) Biogenesis of transport intermediates in the endocytic pathway. FEBS Lett. **452**, 61–66
2 Shaw, J. D., Cummings, K. B., Huyer, G., Michaelis, S. and Wendland, B. (2001) Yeast as a model system for studying endocytosis. Exp. Cell Res. **271**, 1–9
3 Rupper, A. and Cardelli, J. (2001) Regulation of phagocytosis and endo-phagosomal trafficking pathways in *Dictyostelium discoideum*. Biochim. Biophys. Acta **1525**, 205–216
4 Hacker, U., Albrecht, R. and Maniak, M. (1997) Fluid-phase uptake by macropinocytosis in *Dictyostelium*. J. Cell Sci. **110**, 105–112
5 Maniak, M., Rauchenberger, R., Albrecht, R., Murphy, J. and Gerisch, G. (1995) Coronin involved in phagocytosis: dynamics of particle-induced relocalization visualized by a green fluorescent protein tag. Cell **83**, 915–924
6 Adessi, C., Chapel, A., Vincon, M., Rabilloud, T., Klein, G., Satre, M. and Garin, J. (1995) Identification of major proteins associated with *Dictyostelium discoideum* endocytic vesicles. J. Cell Sci. **108**, 3331–3337
7 Journet, A., Chapel, A., Jehan, S., Adessi, C., Freeze, H., Klein, G. and Garin, J. (1999) Characterization of *Dictyostelium discoideum* cathepsin D. J. Cell Sci. **112**, 3833–3843
8 Aguado-Velasco, C. and Bretscher, M. S. (1999) Circulation of the plasma membrane in *Dictyostelium*. Mol. Biol. Cell **10**, 4419–4427
9 Aubry, L., Klein, G., Martiel, J. L. and Satre, M. (1993) Kinetics of endosomal pH evolution in *Dictyostelium discoideum* amoebae. Study by fluorescence spectroscopy. J. Cell Sci. **105**, 861–866
10 Padh, H., Ha, J., Lavasa, M. and Steck, T. L. (1993) A post-lysosomal compartment in *Dictyostelium discoideum*. J. Biol. Chem. **268**, 6742–6747
11 Laurent, O., Bruckert, F., Adessi, C. and Satre, M. (1998) In vitro reconstituted *Distyostelium discoideum* endosome fusion is regulated by Rab7 but proceeds in the absence of ATP-Mg2+ from the bulk solution. J. Biol. Chem. **273**, 793–799
12 Lenhard, J. M., Mayorga, L. and Stahl, P. D. (1992) Characterization of endosome-endosome fusion in a cell-free system using *Dictyostelium discoideum*. J. Biol. Chem. **267**, 1896–1903
13 Souza, G. M., Mehta, D. P., Lammertz, M., Rodriguez-Paris, J., Wu, R., Cardelli, J. A. and Freeze, H. H. (1997) *Dictyostelium* lysosomal proteins with different sugar modifications sort to functionally distinct compartments. J. Cell Sci. **110**, 2239–2248
14 Rauchenberger, R., Hacker, U., Murphy, J., Niewohner, J. and Maniak, M. (1997) Coronin and vacuolin identify consecutive stages of a late, actin-coated endocytic compartment in *Dictyostelium*. Curr. Biol. **7**, 215–218
15 Jenne, N., Rauchenberger, R., Hacker, U., Kast, T. and Maniak, M. (1998) Targeted gene disruption reveals a role for vacuolin B in the late endocytic pathway and exocytosis. J. Cell Sci. **111**, 61–70
16 Antonny, B. and Schekman, R. (2001) ER export: public transportation by the COPII coach. Curr. Opin. Cell Biol. **13**, 438–443
17 Sollner, T., Whiteheart, S. W., Brunner, M., Erdjument-Bromage, H., Geromanos, S., Tempst, P. and Rothman, J. E. (1993) SNAP receptors implicated in vesicle targeting and fusion. Nature (London) **362**, 318–324
18 Rothman, J. E. (1994) Mechanisms of intracellular protein transport. Nature (London) **372**, 55–63
19 Pfeffer, S. R. (1999) Transport-vesicle targeting: tethers before SNAREs. Nat. Cell Biol. **1**, E17–E22
20 Lupashin, V. V. and Waters, M. G. (1997) t-SNARE activation through transient interaction with a rab-like guanosine triphosphatase. Science **276**, 1255–1258
21 Sogaard, M., Tani, K., Ye, R. R., Geromanos, S., Tempst, P., Kirchhausen, T., Rothman, J. E. and Sollner, T. (1994) A rab protein is required for the assembly of SNARE complexes in the docking of transport vesicles. Cell **78**, 937–948
22 Sollner, T., Bennett, M. K., Whiteheart, S. W., Scheller, R. H. and Rothman, J. E. (1993) A protein assembly-disassembly pathway in vitro that may correspond to sequential steps of synaptic vesicle docking, activation, and fusion. Cell **75**, 409–418
23 Kasai, K. and Akagawa, K. (2001) Roles of the cytoplasmic and transmembrane domains of syntaxins in intracellular localization and trafficking. J. Cell Sci. **114**, 3115–3124
24 Campbell, J. L. and Schekman, R. (1997) Selective packaging of cargo molecules into endoplasmic reticulum-derived COPII vesicles. Proc. Natl. Acad. Sci. U.S.A. **94**, 837–842
25 Weidenhaupt, M., Bruckert, F. and Satre, M. (1998) Identification of the *Dictyostelium discoideum* homolog of the N-ethylmaleimide-sensitive fusion protein. Gene **207**, 53–60
26 Weidenhaupt, M., Bruckert, F., Louwagie, M., Garin, J. and Satre, M. (2000) Functional and molecular identification of novel members of the ubiquitous membrane fusion proteins α- and γ-SNAP (soluble N-ethylmaleimide-sensitive factor-attachment proteins) families in *Dictyostelium discoideum*. Eur. J. Biochem. **267**, 2062–2070
27 Bogdanovic, A., Bruckert, F., Morio, T. and Satre, M. (2000) A syntaxin 7 homologue is present in *Dictyostelium discoideum* endosomes and controls their homotypic fusion. J. Biol. Chem. **275**, 36691–36697

28 Watts, D. J. and Ashworth, J. M. (1970) Growth of myxameobae of the cellular slime mould *Dictyostelium discoideum* in axenic culture. Biochem. J. **119**, 171–174

29 Harlow, H. and Lane, D. (1988) Antibodies: A Laboratory Manual, Cold Spring Harbor Laboratory, Cold Spring Harbor, NY

30 Balch, W. E. and Rothman, J. E. (1985) Characterization of protein transport between successive compartments of the Golgi apparatus: asymmetric properties of donor and acceptor activities in a cell-free system. Arch. Biochem. Biophys. **240**, 413–425

31 Rodriguez-Paris, J. M., Nolta, K. V. and Steck, T. L. (1993) Characterization of lysosomes isolated from *Dictyostelium discoideum* by magnetic fractionation. J. Biol. Chem. **268**, 9110–9116

32 Beinert, H. (1978) Micro methods for the quantitative determination of iron and copper in biological material. Methods Enzymol. **54**, 435–445

33 Fasshauer, D., Sutton, R. B., Brunger, A. T. and Jahn, R. (1998) Conserved structural features of the synaptic fusion complex: SNARE proteins reclassified as Q- and R-SNAREs. Proc. Natl. Acad. Sci. U.S.A. **95**, 15781–15786

34 Fukuda, R., McNew, J. A., Weber, T., Parlati, F., Engel, T., Nickel, W., Rothman, J. E. and Sollner, T. H. (2000) Functional architecture of an intracellular membrane t-SNARE. Nature (London) **407**, 198–202

35 Parlati, F., McNew, J. A., Fukuda, R., Miller, R., Sollner, T. H. and Rothman, J. E. (2000) Topological restriction of SNARE-dependent membrane fusion. Nature (London) **407**, 194–198

36 Weimbs, T., Mostov, K., Low, S. H. and Hofmann, K. (1998) A model for structural similarity between different SNARE complexes based on sequence relationships. Trends Cell Biol. **8**, 260–262

37 Antonin, W., Fasshauer, D., Becker, S., Jahn, R. and Schneider, T. R. (2002) Crystal structure of the endosomal SNARE complex reveals common structural principles of all SNAREs. Nat. Struct. Biol. **9**, 107–111

38 Wade, N., Bryant, N. J., Connolly, L. M., Simpson, R. J., Luzio, J. P., Piper, R. C. and James, D. E. (2001) Syntaxin 7 complexes with mouse Vps10p tail interactor 1b, syntaxin 6, vesicle-associated membrane protein (VAMP)8, and VAMP7 in b16 melanoma cells. J. Biol. Chem. **276**, 19820–19827

39 Mullock, B. M., Smith, C. W., Ihrke, G., Bright, N. A., Lindsay, M., Parkinson, E. J., Brooks, D. A., Parton, R. G., James, D. E., Luzio, J. P. and Piper, R. C. (2000) Syntaxin 7 is localized to late endosome compartments, associates with Vamp 8, and is required for late endosome-lysosome fusion. Mol. Biol. Cell **11**, 3137–3153

40 Ward, D. M., Pevsner, J., Scullion, M. A., Vaughn, M. and Kaplan, J. (2000) Syntaxin 7 and VAMP-7 are soluble N-ethylmaleimide-sensitive factor attachment protein receptors required for late endosome-lysosome and homotypic lysosome fusion in alveolar macrophages. Mol. Biol. Cell **11**, 2327–2333

41 Galli, T., Zahraoui, A., Vaidyanathan, V. V., Raposo, G., Tian, J. M., Karin, M., Niemann, H. and Louvard, D. (1998) A novel tetanus neurotoxin-insensitive vesicle-associated membrane protein in SNARE complexes of the apical plasma membrane of epithelial cells. Mol. Biol. Cell **9**, 1437–1448

42 Antonin, W., Holroyd, C., Fasshauer, D., Pabst, S., Von Mollard, G. F. and Jahn, R. (2000) A SNARE complex mediating fusion of late endosomes defines conserved properties of SNARE structure and function. EMBO J. **19**, 6453–6464

43 Advani, R. J., Yang, B., Prekeris, R., Lee, K. C., Klumperman, J. and Scheller, R. H. (1999) VAMP-7 mediates vesicular transport from endosomes to lysosomes. J. Cell Biol. **146**, 765–776

44 Wong, S. H., Zhang, T., Xu, Y., Subramaniam, V. N., Griffiths, G. and Hong, W. (1998) Endobrevin, a novel synaptobrevin/VAMP-like protein preferentially associated with the early endosome Mol. Biol. Cell **9**, 1549–1563

45 Coco, S., Raposo, G., Martinez, S., Fontaine, J. J., Takamori, S., Zahraoui, A., Jahn, R., Matteoli, M., Louvard, D. and Galli, T. (1999) Subcellular localization of tetanus neurotoxin-insensitive vesicle-associated membrane protein (VAMP)/VAMP7 in neuronal cells: evidence for a novel membrane compartment. J. Neurosci. **19**, 9803–9812

46 Martinez-Arca, S., Alberts, P., Zahraoui, A., Louvard, D. and Galli, T. (2000) Role of tetanus neurotoxin insensitive vesicle-associated membrane protein (TI-VAMP) in vesicular transport mediating neurite outgrowth. J. Cell Biol. **149**, 889–900

47 Lafont, F., Verkade, P., Galli, T., Wimmer, C., Louvard, D. and Simons, K. (1999) Raft association of SNAP receptors acting in apical trafficking in Madin-Darby canine kidney cells. Proc. Natl. Acad. Sci. U.S.A. **96**, 3734–3738

48 Hibi, T., Hirashima, N. and Nakanishi, M. (2000) Rat basophilic leukemia cells express syntaxin-3 and VAMP-7 in granule membranes. Biochem. Biophys. Res. Commun. **271**, 36–41

49 Thompson, J. D., Higgins, D. G. and Gibbons, T. J. (1994) CLUSTAL W: improving the sensitivity of progressive multiple sequence alignment through sequence weighting, position-specific gap penalties and weight matrix choice. Nucleic Acids Res. **22**, 4673–4680

Received 29 May 2002/2 August 2002; accepted 13 August 2002
Published as BJ Immediate Publication 13 August 2002, DOI 10.1042/BJ20020845